Journal of Materials Chemistry A

Accepted Manuscript

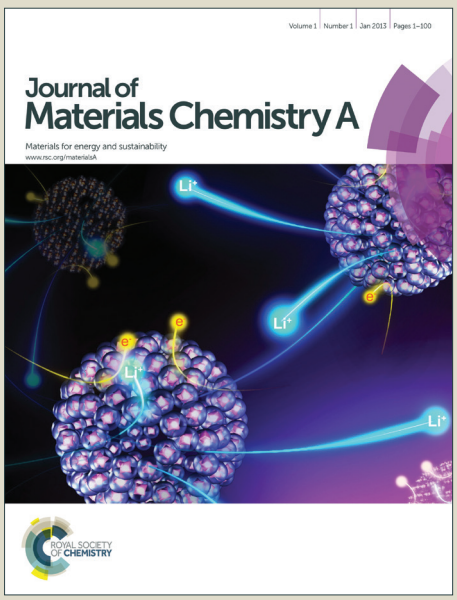

ROYAL SOCIETY OF CHEMISTRY

www.rsc.org/materialsA

Cite this: DOI: 10.1039/c0xx00000x

www.rsc.org/xxxxxx

ARTICLE TYPE

Novel Nitrogen-rich Porous Carbon Spheres as a High-performance Anode Material for Lithium-Ion Batteries

Dongdong Li[a], Liang-Xin Ding,*[a] Hongbin Chen[a], Suqing Wang[a], Zhong Li[a], Min Zhu[b], and Haihui Wang*[a]

Received (in XXX, XXX) Xth XXXXXXXXX 20XX, Accepted Xth XXXXXXXXX 20XX

DOI: 10.1039/b000000x

Carbonaceous materials with suitable structure and component are highly desirable for the development of lithium ion batteries (LIBs), since they can produce the best possible result uniting advantages of various structures and different components. To this end, here a novel nitrogen-rich porous carbon spheres (N-PCS) with appropriate pores distribution are proposed and prepared by using a template-assisted self-assembly method. The as-prepared N-PCS possess high content of instinctive nitrogen and exhibit interconnected sphere structure with quantities of mesopores. As expected, the N-PCS display superior electrochemical performances, such as high initial columbic efficiency (>60%), super cycle stability (retain 540 mA h g^{-1} after 100 cycles at 0.5 A g^{-1}), and good rate capability (215 mA h g^{-1} at 3 A g^{-1}), showing a great promising anode material for the next generation LIBs.

Introduction

Lithium ion batteries (LIBs) as the most promising power batteries are at the heart of technologies in developing pure electric vehicles (PEV) for their highest energy density among the traditional second batteries[1, 2]. Currently, graphite is the main commercial anode material in virtue of its low cost, long lifespan and high initial coulombic efficiency, however, the low theoretical specific capacity (372 mAh g^{-1}) and limited rate capability make it can't meet the ever-increasing demand of PEV[3, 4]. Therefore, a lot of new materials with high energy density and rate capability, such as transition metal oxide[5, 6], lithium alloys[7, 8], non-graphite carbon materials[9, 10], and their composites[11, 12], have been studied as alternative anode materials. Among them, non-graphite carbon materials are regarded as the most promising alternative due to their excellent cycling ability, environment friendly, and resource abundance.

Recently, doping of nitrogen into the carbon crystal lattice has been proved to be an efficient approach to improve the lithium storage capacity for the non-graphite carbon materials[13-16]. Cui and co-workers successfully prepared nitrogen doped graphene nanosheets which showed a higher reversible capacity and a better rate capacity in comparison with graphene nanosheet[15]. The doping of nitrogen could increase the lithium ion adsorption energies and generate plenty of defects which are of benefit to enhance the lithium storage[17-19]. In addition, the presence of N atoms at the carbon surface can enhance the reactivity and electric conductivity which are in favour of the rate capacity[10, 13]

Decreasing of the transport length of lithium ion on the carbon material is another attractive approach to further improve the electrochemical performance, especially rate capability, due to the low solid-state diffusion coefficient of lithium in the carbon materials[20]. Thus, a large number of nano carbon materials with various microstructures have been investigated in the past five years, such as nanofibers[10, 21], nanoparicles[22], nanosheets[23], nanotubes[24, 25], and porous carbons[9, 26-30]. Among them, porous carbons are of particular interest in providing high rate performance because their unique structure could shorten the transport length of lithium ions and enhance the electrolyte diffusion in the carbon electrode. For instance, Song et al. prepared carbon nanosheets with different pore structures. They found that the reversible capacities ascend with the increase of pore content and the best capacity is as high as 355 mAh g^{-1} at the current density of 1 A g^{-1}.[30] Furthermore, to further enhance their electrochemical performance, lots of work has been done to exploit the synergetic effect between porous structure and doping of nitrogen[10, 14, 16]. For example, mesocarbon microbead oxide (MCMBO) modified by nitrogen doping exhibited a higher reversible capacity (762 mAh g^{-1}) compared to the MCMBO (289 mAh g^{-1}) at the same current density.[16] Similarly, Li et al. found that a high reversible capacity of 213 mAh g^{-1} even at the rate of 3 A g^{-1} can be achieved by the nitrogen-doped porous carbon.[14] In these researches, the rate performances have a great improvement by virtue of the doping of nitrogen and their porous structure. However, the porous structure usually contributes to large specific surface area which could lead to low initial coulombic efficiency.[27, 29] How to simultaneously achieve high rate capability and relatively high initial coulombic efficiency is still a challenge. As we known, the micropores are an important contributor to the specific surface area, but it could not effectively improve the electrolyte penetration and ionic diffusion in the carbon material[28, 31, 32]. Therefore, it is highly possible to develop promising anode materials with high rate capability and relatively high initial coulombic efficiency by constructing new porous carbon materials with as low as possible micropores.

Based on the above considerations, here we design and prepare a novel nitrogen-rich porous carbon (N-PCS) with appropriate porous structure by using SiO_2 as the occupying position template. The low content of micropores results in low specific surface area which is of benefit to enhance the initial coulombic efficiency. On the other hand, the abundant mesopores were introduced to shorten the transport length of lithium ion and facilitate liquid electrolyte diffusion. Besides, the high content of instinctive nitrogen could create quantities of lithium ion storage site and enhance the electric conductivity of amorphous carbon. Therefore, it could be expected that the N-PCS possess relatively high initial coulombic efficiency, good rate capability and stable cycling performance.

Experimental

Materials synthesis

All chemical reagents used in this work were analytical grade. The N-PCS were prepared using pyrrole (Py, Aladdin Industrial Corporation) as the precursor, SiO_2 (Aladdin Industrial Corporation) as the template, Sodium dodecyl sulfate (SDS) as the surface active agent, and $FeCl_3 \cdot 6H_2O$ as the initiating agent. As show in the Scheme 1, firstly, 0.05 g SDS and 0.2g SiO_2 were dispersed into deionized water (500 mL) by magnetic stirring for 100 min at the room temperature. Then, 0.5 mL Py was added under vigorous stirring after the above solution cooled down to 0-5 °C in refrigerator. Subsequently, 10 mL $FeCl_3$ (0.07 mol / L) was added to initiate the polymerization reaction of Py. The reaction was carried out for 180 min under magnetic stirring. A black precipitate (PPy@SiO_2) was obtained. The precipitate was washed with deionized water and alcohol until the filtrate became neutral. The as-prepared precipitate was thermolysised at 700 °C for 60min under a nitrogen atmosphere. Finally, the SiO_2 was removed by 10 wt.% HF for 4h with stirring. The N-PCS was obtained after washing with deionized water and drying at 80 °C in an oven for 12h.

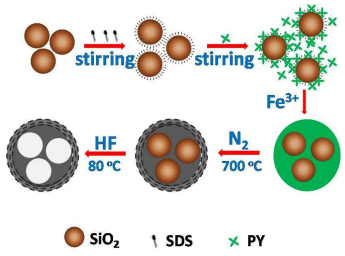

Scheme 1. Schematic illustration of the synthesis of N-PCS

Materials characterization

The morphologies of the N-PCS were examined by field-emission scanning electron microscopy (SEM, Nova NanoSEM 430) and transmission electron microscopy (TEM, JEM-2010). Chemical-state analysis was carried out by X-ray photoelectron spectroscopy (XPS, ESCALAB 250). The structure was characterized by X-ray diffraction (XRD, Bruker D8 Advance) and Raman spectra (LabRAM Aramis). The BET specific surface area, pore size distribution, and total pore volume were obtained from nitrogen sorption measurements (Micromeritics analyzer ASAP 2010 (USA)).

Electrochemical measurements

The electrochemical performance of the N-PCS was tested in a half cell (CR2025) by galvanostatic cycling and cyclic voltammetry at room temperature. The working electrodes were prepared by slurry casting on a Cu foil. The slurry contained 80 wt% active materials, 10 wt% super P, and 10 wt% polyvinylidene (PVDF) binder. The electrodes were separated by celgard 2325 membrane and liquid electrolyte mixtures containing 1 mol L^{-1} $LiPF_6$ and a solvent mixture of ethylene carbonate (EC) and diethyl carbonate (DMC) (1:1 by volume) (Beijing Institute of Chemical Reagents, China). The cells were galvanostatical discharged and charged with the voltage between 0.01 and 3.0 V vs. Li/Li^+ using a Battery Testing System (Neware Electronic Co., China). Cyclic voltammetry (CV) curves were measured at a scanning rate of 0.2 mV s^{-1} within the potential range of 0.01-3.0 V vs. Li/Li^+ using an electrochemistry working station (Zahner IM6ex).

Results and discussion

N-PCS were prepared via template-assisted method as shown in Scheme 1. PPy@SiO_2 nanocomposites were firstly synthesized through in-situ polymerization method, and then the PPy evolved into nitrogen-rich carbon through a thermal treatment approach. At last, the templates were removed and the final products were obtained. The details of the fabrication are described in the experimental section. The as-prepared product was firstly examined by Raman spectroscopy, and the pristine PPy was tested for comparison, as shows in Figure 1a, It can be clearly seen that the characteristic peaks of PPy disappeared after a thermal treatment at 700 °C for 1 h, leaving only the two peaks located at 1587 and 1342 cm^{-1}, which should be corresponded to graphitic band (G) and disordered band (D), respectively.[23, 33, 34] This contrastive result supports that the PPy has been successfully carbonized. In addition, it has been demonstrated that G band is associated to the formation of sp^2 carbon and D band is associated with the disordered or imperfect structures of carbon material.[33, 34] Generally, the intensity ratio of D band to G band (D/G) is usually used to estimate the disorder degree of carbon. For the N-PCS, the intensity ratio of D/G is about 1.19 which is larger than other reports about amorphous carbon[14, 16, 23, 30, 32, 35] and close to the ratio reported for graphene materials[13, 15, 36]. The result shows that the N-PCS have a higher disorder degree than other amorphous carbon. The improved disorder degree of N-PCS may be related to the precursor of the N-PCS. In detail, the nitrogen content of the PPy is more than 20 % and the distribution of nitrogen atom is uniform. As a result, the instinctive nitrogen atom may prevent the formation of sp^2 carbon and promote the growing of imperfect structure during the carbonization process. The high disorder structure of N-PCS could be further confirmed by XRD. From the Figure 1b, it is can be seen that the N-PCS have a very broad and wide peak at 24.7 which is lower than the diffraction angle of graphite, suggesting the amorphous carbon structure of N-PCS.

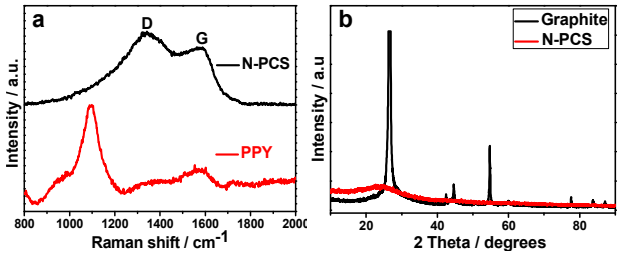

Figure 1. (a) Raman spectra of N-PCS and PPy, (b) XRD patterns of N-PCS and Graphite.

To analyze the elemental composition and bonding configurations, XPS was performed on the as-prepared product. As show in Figure 2a, the survey spectrum of the N-PCS show that only C, N and O are contained and there is no peak of Si, indicating that the SiO_2 have been completely removed by HF. In addition, the result indicates that the mass percentage of doped nitrogen as high as 5.43% of product. Figure 2b shows the N1s spectrum, which can be deconvoluted into three individual peaks, locating at 398.4, 399.7 and 400.9 eV correspond to pyridinic, pyrrolic, and graphitic nitrogen, respectively.[22, 37] The high nitrogen content in the carbon materials is benefitial to the formation of defects and the enhancement of electric conductivity which both can enhance the electrochemical performance of anode materials.

The microstructure of the as-prepared materials was examined by SEM, as show in Figure 3a, the product exhibits spherical

morphology with the diameters in range of 50-100 nm. In addition, these nanoparticles are interconnected with each other. The morphology and structure of the as-synthesized N-PCS were further investigated by TEM. Figure 3b shows the TEM image of the product revealing the porous structure of spheres. More remarkable, there is more than one pore in the sphere which is quite different from the hollow structure sphere. Moreover, the diameters of pores are in the range of 20-30 nm which are equal to the diameters of the SiO_2. It is accepted that the pores are formed during the removal of SiO_2 nanoparticles. Therefore, from the above structure analysis, it is certain that interconnected nitrogen-rich carbon spheres with quantities of mesopores have been successfully prepared. The unique mesopores are ideal electrolyte diffusion channel and interconnection feature are of benefit to the electric transport compared to the granular carbons.[9, 31, 32.]

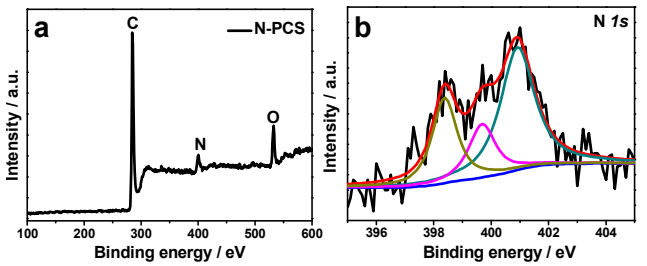

Figure 2. XPS spectra of the N-PCS: survey (a) and N1s (b).

To further examine the porous structure of N-PCS, nitrogen adsorption-desorption isotherms were measured. The Brunauer–Emmett-Teller (BET) surface area of N-PCS is 67.4 m^2 g^{-1}. The hysteresis loops could be observed in the relative pressure of P/P_0 =0.8-0.98 from the N_2 adsorption-desorption isotherm (Figure 4a), which confirmed the existence of mesopores and macropores. [38-40] It is acceptable that the mesopores (20-50 nm) appear during the removal of templates which have been proved by the TEM image, and the macropores are caused by the interconnection and stacking of the carbon spheres. As reported by previous articles, the mesopores and macropores, could provide ideal transport pathways for lithium ion to improve the rate capability. In addition, the unobvious adsorption at low relative pressure (P/P_0 < 0.1) forebodes the low content of the micropores (1-2 nm). Figure 4b shows the pore size distribution curve, exhibiting that the as-prepared products have low content of micropores, and quantities of mesopores and macropores. The small quantity of micropores originates from the pyrolysis process of PPy and is unavoidable in organic matter pyrolysis. The total pore volume is 0.138 cm^3 g^{-1} and microporous volume is just 0.005 cm^3 g^{-1}. The low content of micropores is benefitial to reduce the initial irreversible capacities. Therefore, the N-PCS is expected to have desirable electrochemical properties.

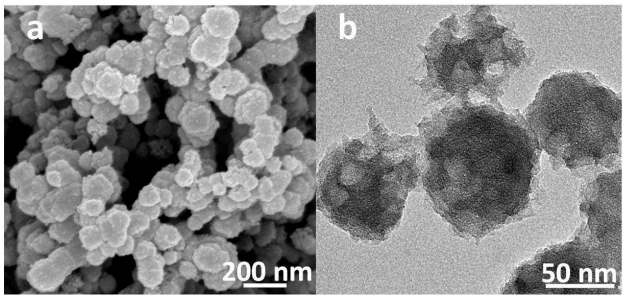

Figure 3. SEM (a) and TEM (b) of N-PCS

The electrochemical performances of the as-prepared N-PCS as anode material were investigated in a half-cell configuration at the current rate of 0.5 A g^{-1} in the voltage range of 0.01−3.0 V (vs Li^+/Li). The result is presented in Figure 5. As shown in Figure 5a, the shape of initial three charge/discharge cycles curves are similar to those previously reported.[21, 22, 25] There is a visible broad plateau at 0.9-0.75 V in the first discharge process. However, the broad plateau at 0.9-0.75 V disappeared in the following cycles. It is acceptable that the above phenomenon is due to the formation of solid electrolyte interphase (SEI) film and other side reactions in the first discharge process.[9, 22] Notably, the initial reversible capacity is as high as 666 mAh g^{-1} at the current density of 0.5 A g^{-1}, which is higher than the theoretical capacity

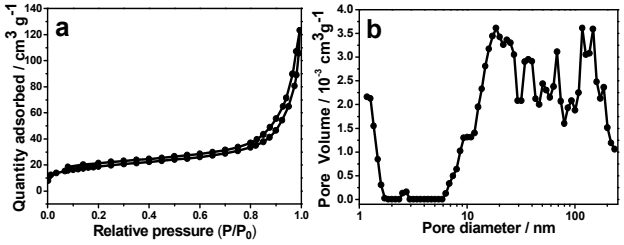

Figure 4. (a) N_2 adsorption/desorption isotherms of N-PCS, (b) Porosity distribution by original density functional theory model.

of graphite (372 mAh g^{-1}) and also higher than those of N-carbon materials.[14, 16, 22] The high reversible capacity might be related to the instinctive nitrogen which creates more Li^+ storage sites. In addition, the N-PCS possess higher content of mesopores and macropores compared to other N-carbon. The quantities of mesopores and macropores could increase the lithium storage at high potential.[30] To further study the discharge and charge process, the cyclic voltammetry (CV) test was conducted at a scanning rate of 0.2 mV s^{-1} within the potential range of 0.01-3.0 V vs. Li/Li^+. The first three cycle curves are showed in Figure 5b. During the first cathodic scan, N-PCS anode exhibits a cathodic peak at about 0.75 V which may correspond to the formation of SEI film.[21, 41] In the subsequent cycles, the reduction peak at about 0.75 V disappears. The phenomenon is in good qualitative agreement with the charge/discharge cycles curves. Furthermore, the peak at above 0-0.5V could be attributed to the lithium ion intercalating into the N-PCS. In the anodic scans, one broad oxidation peak is observed at 1.2 V, which is related to the delithiation of carbon materials.[14, 21]

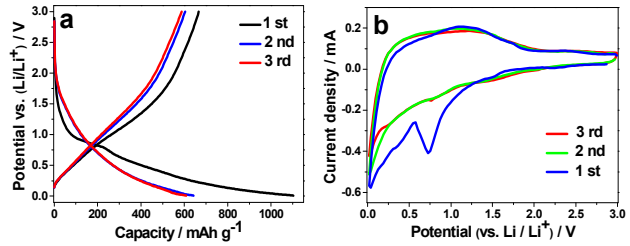

Figure 5. (a) Discharge and charge voltage profiles of the N-PCS at the current density of 0.5 A g^{-1}, (b) CV curves of the N-PCS at a scan rate of 0.2 mV s^{-1}.

Figure 6a displays the cycling performance and coulombic efficiency of the N-PCS electrode at the current density of 0.5 A g^{-1} in the voltage range of 0.01-3.0 V. The N-PCS electrodes show excellent cycle stability compared to other nitrogen-doped carbon nanomaterials.[10, 14, 22] The initial reversible capacity is as high as 631 mAh g^{-1} which decreases fast in the following few

cycles, and then the reversible capacity stabilizes. After 100 cycles, the reversible capacity is as high as 540 mA h g^{-1} and capacity retention is 85.6% compared to the initial reversible capacity which is quite impressive. The low initial coulombic efficiency is common for amorphous carbon, which is mainly caused by the formation of SEI film in the first discharge process.[22, 30] In our work, the initial coulombic efficiency is as high as 64% which is higher than those of the reported N-carbons.[10, 14, 16, 22] The phenomenon may be attributed to its low specific surface area. Lower specific surface area usually can reduce the initial irreversible capacities. Moreover, the coulombic efficiency maintains above 99% after ten cycles, indicating the excellent cycle stability of the N-PCS. Its favourable cycle performances can be ascribed to the unique interconnected and porous structure which provides strain relaxation during Li^+ insertion/disinsertion, and suitable specific surface area which is important for reduction of the decomposition of electrolyte during cycling.

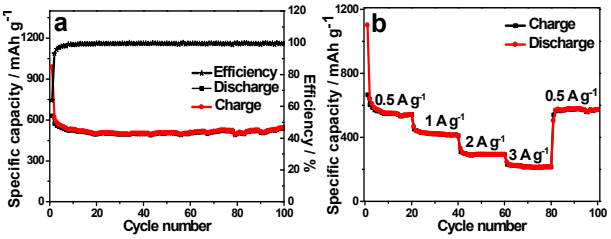

Figure 6. (a) Cycle performance of N-HPCS at the current density of 0.5 A g^{-1}, (b) at various current densities of 0.5, 1, 2 and 3 A g^{-1}. All carried out in the voltage range 0.01-3.0 V vs. Li/Li^+.

Besides the high cycle stability, the N-PCS also exhibit promisingly high rate performance. Figure 6b shows the rate capability of the N-PCS at various current densities from 0.5 to 3 A g^{-1} and then revert back to 0.5 A g^{-1} each for 20 cycles. The reversible capacities are 542, 410, 293, and 215 mA h g^{-1} at 0.5 (1.34C), 1 (2.69C), 2(5.38C) and 3 A g^{-1}(8.06C), respectively. The rate performance of the N-PCS electrode is excellent when comparing to other reports. Zhang et al.[9] prepared hollow carbon nanospheres whose reversible capacity is only 229 mAh g^{-1} at the rate of 5C. Yu et al.[22] reported the nitrogen-doped carbon nanoparticles, whose capacity is just about 300 mAh g^{-1} at the current density of 372 mA g^{-1}. The super rate performance of N-PCS anode can be attributed to the synergetic effect between its structure and instinctive high nitrogen content. More specifically, the mesoporous structure could offer a large electrode/electrolyte interface and shorten the transport length of lithium ion, the interconnected carbon nanoparticles are benefitial to the conduction of electron, and the instinctive nitrogen creates more lithium ion storage sites and further enhances the electronic conductivity. All of them are important for the improvement of the rate performance of the electrode materials. When the current density is tuned back to 0.5 A g^{-1} after cycling at different rates, the specific capacity can be recovered to 570 mAh g^{-1} after 100 cycles, implying the good reversibility and high stability of the materials which benefits from its interconnected and porous structure.

Conclusion

In summary, the N-PCS with appropriate pores distribution have been successfully prepared by a facile approach using SiO_2 as the template and pyrrole as the precursor. The as-synthesized N-PCS used as an anode material for LIBs exhibited a large reversible lithium storage capacity (540 mAh g^{-1} in the 100th cycle at 0.5 A g^{-1}) and superior rate capability (215 mAh g^{-1} when the discharge current enlarged from 0.5 A g^{-1} to 3 A g^{-1}), showing a great promising anode material for high-performance LIBs. The super electrochemical performances should originate from its unique interconnected sphere structure, appropriate pores distribution, and high instinctive nitrogen content, which endow a shorter lithium-ion diffusion length, and more lithium-storage sites. Furthermore, due to the high nitrogen content and the modified pore structure, the N-PCS are also a potential material for application in catalysis, supercapacitors, and hydrogen storage.

Acknowledgements

This work was supported by National Science Fund for Distinguished Young Scholars of China (no. 21225625) and the Pearl River Scholar Program of Guangdong Province.

Notes and references

[a] School of Chemistry & Chemical Engineering, South China University of Technology, Guangzhou 510640 (China). Fax: (+86)20-87110131; E-mail: lxding@scut.edu.cn, hhwang@scut.edu.cn

[b] School of Materials Science and Engineering, Key Laboratory of Advanced Energy Storage Materials of Guangdong Province, South China University of Technology, Guangzhou 510640 (China)

1. M. Armand and J. M. Tarascon, *Nature*, 2008, **451**, 652-657.
2. J. M. Tarascon and M. Armand, *Nature*, 2001, **414**, 359-367.
3. J. B. Goodenough and Y. Kim, *Chem. Mater.*, 2010, **22**, 587-603.
4. M. R. Palacin, *Chem. Soc. Rev.*, 2009, **38**, 2565-2575.
5. P. Poizot, S. Laruelle, S. Grugeon, L. Dupont and J. M. Tarascon, *Nature*, 2000, **407**, 496-499.
6. D. Li, L.-X. Ding, S. Wang, D. Cai and H. Wang, *J. Mater. Chem. A*, 2014, **2**, 5625-5630.
7. J. Qin, C. N. He, N. Q. Zhao, Z. Y. Wang, C. S. Shi, E. Z. Liu and J. J. Li, *ACS Nano*, 2014, **8**, 1728-1738.
8. J. Chang, X. Huang, G. Zhou, S. Cui, P. B. Hallac, J. Jiang, P. T. Hurley and J. Chen, *Adv. Mater.*, 2014, **26**, 758-764.
9. F. D. Han, Y. J. Bai, R. Liu, B. Yao, Y. X. Qi, N. Lun and J. X. Zhang, *Adv. Energy Mater.*, 2011, **1**, 798-801.
10. L. Qie, W. M. Chen, Z. H. Wang, Q. G. Shao, X. Li, L. X. Yuan, X. L. Hu, W. X. Zhang and Y. H. Huang, *Adv. Mater.*, 2012, **24**, 2047-2050.
11. M. Zhang, F. Yan, X. Tang, Q. Li, T. Wang and G. Cao, *J. Mater. Chem. A*, 2014, **2**, 5890-5897.
12. P. Lian, J. Wang, D. Cai, L. Ding, Q. Jia and H. Wang, *Electrochim. Acta*, 2014, **116**, 103-110.
13. Z. S. Wu, W. C. Ren, L. Xu, F. Li and H. M. Cheng, *ACS Nano*, 2011, **5**, 5463-5471.
14. X. Li, X. Zhu, Y. Zhu, Z. Yuan, L. Si and Y. Qian, *Carbon*, 2014, **69**, 515-524.
15. H. Wang, C. Zhang, Z. Liu, L. Wang, P. Han, H. Xu, K. Zhang, S. Dong, J. Yao and G. Cui, *J. Mater. Chem.*, 2011, **21**, 5430-5434.
16. P. Han, Y. Yue, L. Zhang, H. Xu, Z. Liu, K. Zhang, C. Zhang, S. Dong, W. Ma and G. Cui, *Carbon*, 2012, **50**,1355-1362
17. C. C. Ma, X. H. Shao and D. P. Cao, *J. Mater. Chem.*, 2012, **22**, 8911-8915.
18. R. Czerw, M. Terrones, J. C. Charlier, X. Blase, B. Foley, R. Kamalakaran, N. Grobert, H. Terrones, D. Tekleab, P. M. Ajayan, W. Blau, M. Ruhle and D. L. Carroll, *Nano Lett.*, 2001, **1**, 457-460.
19. N. Kurita, *Carbon*, 2000, **38**, 65-75.
20. Y. G. Guo, J. S. Hu and L. J. Wan, *Adv. Mater.*, 2008, **20**, 2878-2887.
21. Z. Wang, X. Xiong, L. Qie and Y. Huang, *Electrochim. Acta*, 2013, **106**, 320-326.
22. D. Bhattacharjya, H.-Y. Park, M.-S. Kim, H.-S. Choi, S. N. Inamdar and J.-S. Yu, *Langmuir*, 2014, **30**, 318-324.

23. R. R. Song, H. H. Song, J. S. Zhou, X. H. Chen, B. Wu and H. Y. Yang, *J. Mater. Chem.*, 2012, **22**, 12369-12374.
24. C. de las Casas and W. Z. Li, *J. Power Sources*, 2012, **208**, 74-85.
25. M. Wu, J. Chen, C. Wang, F. Wang and B. Yi, *Electrochim. Acta*, 2013, **105**, 462-467.
26. K. Tang, R. J. White, X. K. Mu, M. M. Titirici, P. A. van Aken and J. Maier, *ChemSusChem*, 2012, **5**, 400-403.
27. J. Yang, X.-y. Zhou, Y.-l. Zou and J.-j. Tang, *Electrochim. Acta*, 2011, **56**, 8576-8581.
28. K. T. Lee, J. C. Lytle, N. S. Ergang, S. M. Oh and A. Stein, *Adv. Funct. Mater.*, 2005, **15**, 547-556.
29. Y. Han, P. Qi, S. Li, X. Feng, J. Zhou, H. Li, S. Su, X. Li and B. Wang, *Chem.Commun.*, 2014. DOI: 10.1039/C4CC02691H
30. R. Song, H. Song, X. Chen, Y. Cui, J. Zhou and S. Zhang, *Electrochim. Acta*, 2014, **127**, 186-192.
31. F. Cheng, Z. Tao, J. Liang and J. Chen, *Chem. Mater.*, 2008, **20**, 667-681.
32. F. Zhang, K.-X. Wang, G.-D. Li and J.-S. Chen, *Electrochem. Commun.*, 2009, **11**, 130-133.
33. A. C. Ferrari and J. Robertson, *Phys. Rev. B*, 2000, **61**, 14095-14107.
34. A. C. Ferrari, J. C. Meyer, V. Scardaci, C. Casiraghi, M. Lazzeri, F. Mauri, S. Piscanec, D. Jiang, K. S. Novoselov, S. Roth and A. K. Geim, *Phys. Rev. Lett.*, 2006, **97**, 187401–187404.
35. B.-S. Lee, S.-B. Son, K.-M. Park, W.-R. Yu, K.-H. Oh and S.-H. Lee, *J. Power Sources*, 2012, **199**, 53-60.
36. P. Lian, X. Zhu, S. Liang, Z. Li, W. Yang and H. Wang, *Electrochim. Acta*, 2010, **55**, 3909-3914.
37. Q. Liu, Z. Pu, C. Tang, A. M. Asiri, A. H. Qusti, A. O. Al-Youbi and X. Sun, *Electrochem. Commun.,* 2013, **36**, 57-61.
38. P. K. Tripathi, M. Liu, Y. Zhao, X. Ma, L. Gan, O. Noonan and C. Yu, *J. Mater. Chem. A*, 2014, **2**, 8534-8544.
39. X. Ma, M. Liu, L. Gan, P. K. Tripathi, Y. Zhao, D. Zhu, Z. Xu and L. Chen, *Phys.Chem.Chem.Phys.*, 2014, **16**, 4135-4142.
40. P. K. Tripathi, L. Gan, M. Liu, X. Ma, Y. Zhao, D. Zhu, Z. Xu, L. Chen and N. N. Rao, *Mater. Lett.* , 2014, **120**, 108-110.
41. K. Tang, R. J. White, X. Mu, M.-M. Titirici, P. A. van Aken and J. Maier, *ChemSusChem*, 2012, **5**, 400-403.

Cite this: DOI: 10.1039/c0xx00000x

www.rsc.org/xxxxxx

ARTICLE TYPE

Table of Contents

Novel Nitrogen-rich Porous Carbon Spheres as a High-performance Anode Material for Lithium-Ion Batteries

Dongdong Li[a], Liang-Xin Ding,*[a] Hongbin Chen[a], Suqing Wang[a], Zhong Li[a], Min Zhu[b], and Haihui Wang*[a]

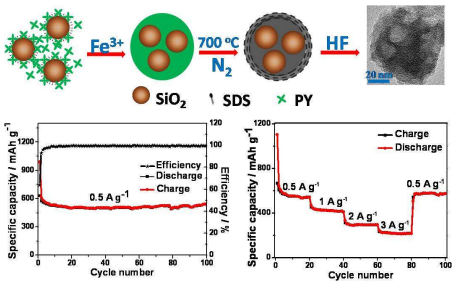

Novel nitrogen-rich porous carbon spheres with appropriate pores distribution are proposed and prepared by using a template-assisted self-assembly method, which exhibit superior electrochemical performance as a promising anode material for LIBs.